

Modelling the efficacy of hyperthermia treatment

Mikołaj Rybiński¹

Institute of Informatics,
University of Warsaw, Warsaw, Poland
and
Mossakowski Medical Research Centre,
Polish Academy of Sciences, Warsaw, Poland

Zuzanna Szymańska

Interdisciplinary Centre for Mathematical and Computational Modelling,
University of Warsaw, Warsaw, Poland

Sławomir Lasota

Institute of Informatics,
University of Warsaw, Warsaw, Poland

Anna Gambin

Institute of Informatics,
University of Warsaw, Warsaw, Poland
and
Mossakowski Medical Research Centre,
Polish Academy of Sciences, Warsaw, Poland

October 15, 2018

¹Corresponding author. Current address: Department of Biosystems Science and Engineering, ETH Zurich, Mattenstrasse 26, 4058 Basel, Switzerland, Tel.: (004161)387-3385, Fax: (004161)387-3994

Abstract

Multimodal oncological strategies which combine chemotherapy or radiotherapy with hyperthermia have a potential of improving the efficacy of the non-surgical methods of cancer treatment. Hyperthermia engages the heat-shock response mechanism (HSR), main component of which are heat-shock proteins (HSP). Cancer cells have already partially activated HSR, thereby, hyperthermia may be more toxic to them relative to normal cells. On the other hand, HSR triggers thermotolerance, i.e. hyperthermia treated cells show an impairment in their susceptibility to a subsequent heat-induced stress. This poses questions about efficacy and optimal strategy of the anti-cancer therapy combined with hyperthermia treatment.

To address these questions, we adapt our previous HSR model and propose its stochastic extension. We formalise the notion of a HSP-induced thermotolerance. Next, we estimate the intensity and the duration of the thermotolerance. Finally, we quantify the effect of a multimodal therapy based on hyperthermia and a cytotoxic effect of bortezomib, a clinically approved proteasome inhibitor. Consequently, we propose an optimal strategy for combining hyperthermia and proteasome inhibition modalities.

In summary, by a proof of concept mathematical analysis of HSR we are able to support the common belief that the combination of cancer treatment strategies increases therapy efficacy.

Key words: heat-shock response; thermotolerance; hyperthermia; proteasome inhibitor; mass action kinetics

Introduction

Most of the non-surgical methods of cancer treatment (e.g. chemotherapy and radiotherapy) are based on the principle of putting some kind of stress on cancer cells to induce their death. Unfortunately, in many cases the above methods fail. The fact that *heat-shock proteins* (HSP) prevent apoptosis induced by different modalities of cancer treatment explains how these proteins could limit the application of such anti-cancer therapies [1]. In order to improve the efficacy of these treatments, some effort is focused on the multimodal oncological strategies which usually combine treatment of chemo- or radiotherapy with hyperthermia.

Heat-shock response in cancer treatment

HSP are a group of highly conserved proteins involved in many physiological and pathological cellular processes. They are so called chaperones, as they protect proteins from stress and help new and distorted proteins with folding into their proper shape [2]. In principle, HSP synthesis increases under stress conditions. Subsequently, upregulation of HSP increases cell survival and stress-tolerance [3]. Elevated expression of different members of HSP family has been detected in several cases of tumour (see, e.g., [4]). Despite its importance, little is still known about how exactly HSP are involved in different processes related to cancer development. In this work we are interested in the heat-shock inducible isoform of heat-shock proteins 70 kDa (Hsp70). For a sake of clarity, we will denote Hsp70 protein by HSP, and use the former only if context might be unclear.

Hyperthermia is a therapeutic procedure used to raise the temperature of a whole body or a region of the body affected by cancer. Body tissues are, globally or locally, exposed to temperatures up to 45°C [5]. Besides characteristics specific to cell type, the effectiveness of hyperthermia depends on the temperature achieved during the treatment, as well as on the length of the treatment [5,6]. In general, moderate hyperthermia treatment, which maintains temperatures in a moderate 40–42°C range for about an hour, does not damage most of normal tissues and has acceptable adverse effects [5, 7].

Currently, hyperthermia effectiveness is under study in clinical trials, including combination with other cancer therapies [5, 7]. A synergistic interaction of radiotherapy and hyperthermia as well as some cytotoxic drugs and hyperthermia has already been confirmed in experimental studies [6]. In particular, Neznanov et al. [8] demonstrated, *in vitro*, that induction of

heat-shock response (HSR) by hyperthermia enhances the efficacy of a proteasome inhibitor called bortezomib — a FDA-approved drug for treatment of a multiple myeloma and mantle cell lymphoma [9]. Basically, hyperthermia engages the HSR mechanism, main component of which are the anti-apoptotic HSP. Cancer cells have already partially activated HSR because they are constitutively coping with higher level of misfolded protein (mainly due to rapid rate of proliferation and specific intracellular conditions of cancer cells). Therefore, in principle, sufficiently increased level of misfolded proteins, as obtained by, e.g., hyperthermia, can not be matched by cell's HSR capacity and, in effect, such enhanced proteotoxic stress can be more toxic to them relative to normal cells [8].

On the other hand, after a heat-shock, all cell types show an impairment in their susceptibility to heat-induced cytotoxicity. This phenomenon, known as *thermotolerance*, is triggered by HSR and it is, at least partially based, on the upregulation of HSP [6]. Thermotolerance is, in principle, reversible and persists for usually between 24 and 48 hours [5]. Due to this phenomenon the applicability of the combined hyperthermia therapy may be, counter-intuitively, initially limited. This naturally poses questions about the efficacy and about an optimal strategy of the hyperthermia treatment.

Our results

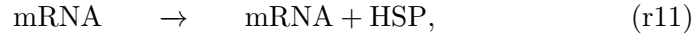
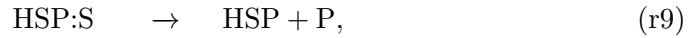
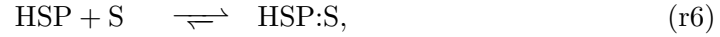
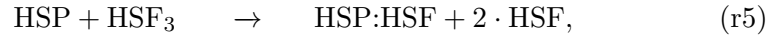
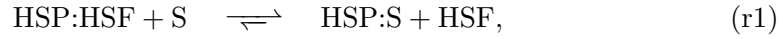
We formalise the notion of the HSP-induced thermotolerance i.e. the memory of the HSR system of the previous temperature perturbation, or, the system desensitisation with respect to the second consecutive heat-shock. Using mathematical modelling we compute the intensity and the duration of the thermotolerance. Finally, we give a quantification of an effect of a combined therapy of hyperthermia and an bortezomib-induced proteasome inhibition. Based on that, we propose an optimal strategy for combination of heat-shock and the inhibitor. In principle, our results support the common belief that the combination of aforementioned cancer treatment strategies increases therapy efficacy.

Model

The main purpose of this work is to contribute to the understanding of the involvement of the HSR mechanism in multimodal cancer therapies. To this end, we use a refined version of our previous deterministic model [10].

Despite of its simplicity it provides a sound qualitative description of the HSR mechanism.

This model captures dynamics of synthesis of HSP and its interactions with key intracellular components of HSR, i.e.: HSP; the *heat-shock factor* (HSF) and its trimer, which is a HSP transcription factor; HSP substrate — mainly denatured, misfolded native proteins; HSP gene — *heat-shock element* (HSE); and HSP mRNA. Fig. 1 depicts the overall model scheme, and following reactions give the precise model structure:



Four out of twelve reactions (Eqs r1–r12) are reversible, making it sixteen reactions in total; T superscript over the reaction arrow denotes temperature dependence. The proteins denaturation level dependence on temperature is modelled by a power-exponential function, analogously to some of the previous HSR mathematical models [10–13]. This type of functional relation is based on an experimental calorimetric enthalpy data [14].

Deterministic mathematical model follows purely mass action kinetics and it is represented by the first order ordinary differential equations (ODE). Fig. 2 depicts behaviour of this model, which starts in the state of homeostasis, i.e. in a steady state for $T = 37^\circ\text{C}$, in response to the immediate shift of the temperature to $T = 42^\circ\text{C}$. Amounts of species are arbitrarily scaled, each of them separately, to obtain values of a similar order of magnitude for each species (denoted a.s.M). We calibrated this model with respect to the HSE:HSF₃ 42°C experimental data [15] (Fig. S2 in the Supporting Material).

We additionally developed a stochastic counterpart of the deterministic model, represented by *chemical master equation* (CME) or, equivalently, *continuous-time Markov process* (CTMC), which we then analysed using the *probabilistic model checking* technique (PMC). To ensure the feasibility of this approach we used approximate PMC techniques, implemented recently in the PRISM tool [16].

We found deterministic approach to be a valid approximation of stochastic model, i.e., both variants presented very similar results with respect to the stochastic mean. However, almost half of the modelled species exhibit a significant noise level in the stochastic model. See Text S3 in the Supporting Material, Sec. 1 for details. Both deterministic and stochastic models are additionally available in the Supporting Material, respectively, as a XML File F1 in the SBML format [17], as well as a text File F2 in the PRISM model format [16].

Results

Quantification of the thermotolerance phenomenon

Thermotolerance can be described as a desensitisation with respect to a consecutive heat-shock, compared to the response to the first heat-shock. In other words, thermotolerance represents a memory of the system about the first two, “on” and “off” temperature perturbations, leading to a decreased response to the subsequent “on” perturbation. In case of the HSR system, its memory is created by a propagating shift in species activity and the feedback loop of the biochemical network (cf. Fig. 2).

Fig. 3 depicts the thermotolerance phenomena in the deterministic HSR model for the immediate 42°C heat-shock. Duration and strength of the memory of the first temperature perturbation can be accurately tracked by the activity of HSP, level of which is negatively correlated with the strength of the response (cf. Fig. S4 in the Supporting Material).

In the stochastic model we introduce approximate perturbations as an independent, k -level Poisson process (see Text S3 in the Supporting Material, Sec. 3 for details). This allows to stay within the same mathematical model, i.e., CTMC, and seamlessly perform stochastic simulations and model checking.

We define the notion of the HSP-induced thermotolerance during n -th heat-shock ($n > 1$) as the *desensitisation coefficient*:

$$\mathcal{D}_n = 1 - \frac{\mathcal{R}_n}{\mathcal{R}_1}, \quad (1)$$

where n -th response \mathcal{R}_n is defined as:

$$\mathcal{R}_n = \max_{t_n \leq t < t_{n+1}} \{\#S(t) - \#S^*\}, \quad (2)$$

where $\#S^* = \mathbb{E}_\pi(\#S)$ is a mean value of a species S amount in a steady state π ; t_n is a n -th heat-shock start time (we assume $t_{n+1} = \infty$ if not specified otherwise); and the first response, by assumption, satisfies $\mathcal{R}_1 > 0$. Such response measure represents the toxicity of the heat-shock: the higher the response the more likely the cell will die. For the deterministic model the species amount is simply a scaled value of ODE variable, corresponding to the mean value of a stochastic process random variable.

Fig. 4 depicts value of the desensitisation coefficient \mathcal{D}_2 for the substrate species, with respect to the time gap between heat-shocks. After the first heat-shock, at the time gap of the approximated memory loss, i.e. at ca. 400 min, system is very close to the homeostasis steady state (cf. Fig. S1 in the Supporting Material, $t \approx \Delta t_1 + 400 \approx 470$ min).

In the stochastic model we may observe a non-zero (slightly positive) level of mean \mathcal{D}_2 , after the thermotolerance effect has vanished. More importantly, the stochastic variant presents a constantly high standard deviation of the desensitisation intensity: ca. 20% of its expected maximum level (which is observed for the very short time gap between heat shocks). These results, as well as the overall difference with respect to the deterministic model, may be attributed to the stochastic noise and the fact that we take a maximum amount of substrate in Eq. 2 to measure its toxic influence, not the mean value.

Hyperthermia in multimodal oncological strategies

It has been hypothesised that because hyperthermia engages HSR mechanism and because capacity of this mechanism is limited, especially in cancer cells, hyperthermia enhances the toxicity induced by a second modality of cancer treatment [8]. This synergistic effect of hyperthermia and other cancer therapies can be attributed to the much higher accumulation of denatured proteins (substrate), which are deadly for cell. In our modelling approach we investigate, by means of the presented mathematical HSR model, the temperature dependence of the heat-shock response in combination with bortezomib-induced inhibition of proteasome.

In our intracellular-level model we assume that hyperthermia treatment is represented by a heat-shock with an immediate temperature shift, as presented in previous section. In order to incorporate into the model the

inhibitory effect of bortezomib, we limit the HSP-assisted degradation of denatured proteins (Eq. r9) and degradation of HSP itself (Eq. r8). More precisely, we linearly scale both reaction rate constants k , i.e., we set $(1-I) \cdot k$, for $I \in [0, 1]$, where I represents current inhibition level (when no drug is administrated $I = 0$ whereas in case of maximum inhibition $I = I_{100}$).

We used bortezomib pharmacodynamics as modelled by Sung & Simon [18]. Namely, the inhibition level linearly raises up to its maximum level at $t_{100}=60$ min, after which it decays with a half-life $t_{50} = 12 \cdot t_{100}$, i.e.:

$$I(t) = I_{100} \cdot \begin{cases} \frac{t}{t_{100}} & \text{for } t \leq t_{100} \\ e^{-k_I(t-t_{100})} & \text{for } t > t_{100} \end{cases}, \quad (3)$$

where $k_I = \ln(2)/t_{50}$. The maximum inhibition level I_{100} directly corresponds to the drug dose. For a maximum tolerated bortezomib dose, I_{100} is equal to ca. 65%, while for some of the next-generation proteasome inhibitors, such as carfilzomib or ONX-0912, both of which are in clinical development, it was possible to reach over 80% proteasome inhibition in blood (with consecutive-day dosing schedules) [9].

Fig. 5 depicts activity of substrate and HSP:substrate complex, with respect to an unimodal proteasome inhibition treatment for a range of its maximum levels I_{100} , as well as a unimodal hyperthermia treatment and combined 65% maximum inhibition treatment for a range of moderate hyperthermia temperatures. Recall that activity peak of a cytotoxic substrate defines level of heat-shock response \mathcal{R}_1 (Eq. 2). The higher the response is the more effective is the therapy in terms of indicating a higher probability of death of a cancer cell.

The bortezomib-based proteasome inhibition and hyperthermia induce a very similar total number of denatured proteins (see Fig. 5). However, in case of proteasome inhibition vast majority of these proteins is being secured in HSP:substrate complexes on the fly. This is due to the gradual increase of bortezomib inhibition effect, which is not fast enough with respect to a rate at which new HSP molecules are synthesised. The immediate heating has a much better effect in terms of substrate cytotoxicity. Furthermore, when both therapies are applied simultaneously levels of both substrate and HSP:substrate complex indeed are higher than in case of an application of only one of the treatment modalities. HSR capacity, as represented by an analogous \mathcal{R}_1 coefficient for HSP:substrate complex (cf. Eq. 2), is much closer to saturation plateau in case of the 65% peak inhibition level than without inhibition (see Fig. 5). Hence, increase of the temperature has a better effect in the combined treatment, in the sense of a deadly accumulation

of free substrate molecules.

Fig. 6 depicts this synergistic effect in a continuous scale of both the temperature and the maximum inhibition level of bortezomib. A monotone increase in response with respect to both modalities can be observed regardless of the heat-shock application time (see Fig. S5 in the Supporting Material). We found that multimodal toxicity response increases by over 40% with respect to a unimodal hyperthermia response for a maximum inhibition level equal to reported 65%, up to over 80% increase for a theoretical maximum of 100% of proteasome inhibition. Moreover, we established $t_1^* \approx 38$ min as an optimal time to start hyperthermia treatment in combination with 65% bortezomib inhibition (see Fig. 6). Interestingly, this is not in agreement with a maximum area under the bortezomib inhibition curve (AUC), a common pharmacokinetic efficacy measure. For the heat-shock duration $\Delta t_1 = 71$ min, AUC maximum is reached at $t_1 \approx 56$ min (see Fig. S6 in the Supporting Material). Timing of heat-shock in the optimal multimodal treatment strategy t_1^* can be intuitively explained by the following observations (cf. Fig. 5). Firstly, time required for denatured proteins to peak after the beginning of a heat-shock is roughly the same as the time gap between t_1^* and t_{100} (22 min). Secondly, at t_1^* the inhibition itself has still a relatively low impact. This way, inhibition peak coincides with the period of maximum temperature-induced toxicity, at which HSR mechanism is the most occupied, thus effecting in the optimal synergistic toxicity.

Conclusions and Discussion

We formalised and quantified the notion of thermotolerance induced by the HSP-based mechanism of heat-shock response. Although we found a deterministic approach to be a valid approximation of the stochastic HSR model, the latter variant presented a high level of intrinsic noise. In consequence, we observe a significant level of intrinsic thermotolerance intensity which can be highly increased by the heat-shock accompanied by a high reduction of variability. We would like to emphasise that in this analysis we demonstrated feasibility and practical potential of the probabilistic model checking technique, more specifically its lesser known approximate variant.

Next, by mathematical modelling of HSR we were able to support the common belief that the combined cancer treatment strategies can more effectively increase cytotoxicity of denatured proteins in cancer cells than unimodal strategies. Moreover, we presented an optimal starting time for a moderate hyperthermia treatment in combination with a proteasome in-

hibitor application. This is an example of how mechanistic modelling can surpass pharmacokinetic measures of optimal drug efficacy, such as AUC (which basically is an optimisation only with respect to system's input).

We suggest that the synergistic effect of hyperthermia and other cancer treatment modalities (like chemo- and radiotherapies) is caused by increased accumulation of denatured proteins, i.e., heat and drug-sensitive proteins or heat and radiation-sensitive proteins. This results in bigger demand for heat-shock proteins and higher selective barrier for cells.

Our model-based analysis proves successful in reproducing experimental knowledge of key aspects of hyperthermia treatment, and as such offers reasonable framework for studying its connections with heat-shock response. However, all of the kinetic models of molecular biological systems and means of their analysis are incomplete due to constraints under which these models are formulated. In this regard, we would like to point out that this is a proof of concept model-based analysis and there are many issues to address within this work. For instance, we omitted the investigation of the day-based strategies of multimodal treatment. This is because we found that in our HSR model the single cell level thermotolerance duration (ca. 6.5h) is much shorter than the bortezomib decay (12h half-life), thus, making the latter a determining factor for a standard, daily dosing schedule. The inconsistency between reported (24-48h) and simulated duration of thermotolerance can be primarily attributed to the fact that thermotolerance, in general, is most likely not only induced by the HSP upregulation (cf. [19]). Secondly, this inconsistency may also be attributed to the simplistic single cell modelling of the immediate temperature shift, disregarding spatial heat distribution and the preheating period as in, e.g., the whole-body hyperthermia (cf. [5]). In this regard, to provide solid, quantitative results, our model requires more extensive calibration with respect to experimental data, including the behaviour for varying temperatures (cf. [10, 20]). Nevertheless, undoubtedly, our analysis gives a valuable mathematical framework for model-based understanding of hyperthermia treatment strategies, such as these combining hyperthermia with very promising therapeutic proteasome inhibitors.

Methods

Model was defined using the SBML-SHORTHAND notation [21], and automatically generated in the SBML format [17]. The ODE model was numerically solved using the MATHSBML package of the MATHEMATICA software [22]. The corresponding stochastic version of this model, represented by

CME or, equivalently, CTMC (cf. [23]), was analysed using the PMC technique. To ensure the feasibility of this approach we have used approximate PMC techniques (APMC), implemented recently in the PRISM tool [16]. Consequently, all stochastic simulations and the confidence interval-based APMC were done using PRISM. To create the PRISM model, we used a prototype SBML translator which generates model specification in the PRISM language. Minor adjustments, such as factorisation of parameters or accounting for mass conservation laws were done manually.

For means of modelling frameworks comparison and stochastic noise quantification (see Text S3 in the Supporting Material, Sec. 1) as well as for thermotolerance quantification (see Fig. 4) we used PRISM rewards to describe first and second moments of, respectively, species variables as well as one minus desensitisation coefficient (see Eq. 1). Text S3 in the Supporting Material, Sec. 2 describes in detail the unbiased estimators and their symmetric confidence intervals for mean, variance, variance-to-mean ratio, and for standard deviation of both species and desensitisation coefficient random variables.

To stay within CTMC framework and, consequently, to seamlessly perform stochastic simulations or model checking, we introduced approximate stochastic perturbation events based on n -counting Poisson processes. Precision of a single perturbation event, measured as a standard deviation, is proportional by square root to the number of counting levels n and inverse linearly proportional to the expected time of occurrence of this event. The approximate stochastic perturbation strategy for on and off heat-shock events was encoded manually in PRISM language, according to the scheme presented in Text S3 in the Supporting Material, Sec. 3.

Acknowledgements

The work of ZS was supported by the Polish National Science Centre grant 2011/01/D/ST1/04133. The work of MR and SL was partially supported by the Polish Ministry of Science and Higher Education grant N N206 356036. The work of MR and AG was partially supported by the Polish National Science Center grant 2011/01/B/NZ2/00864 and by the Biocentrum Ochota project POIG.02.03.00-00-003/09.

MR carried out the case study, prepared all figures and has written the manuscript. ZS and SL prepared parts of the manuscript. ZS participated in model adjustments. SL supervised the model checking experiments. AG supervised the whole project and participated in drafting of the manuscript

and improving of the final manuscript. All authors have read and approved the final manuscript and there is no conflict of interest to declare.

All authors would like to thank to prof. Maciej Żylicz (International Institute of Molecular and Cell Biology in Warsaw) and prof. Bogdan Lesyng (University of Warsaw) for valuable discussions and for inspiring this research.

References

- [1] Mayer, M. P. & Bukau, B. 2005 Hsp70 chaperones: cellular functions and molecular mechanism. *Cell. Mol. Life Sci.* **62**, 670–684.
- [2] Georgopoulos, C. & Welch, W. J. 1993 Role of the major heat shock proteins as molecular chaperones. *Ann. Rev. Cell Biol.* **9**, 601–634.
- [3] Parsell, D. A. & Lindquist, S. 1993 The function of heat-shock proteins in stress tolerance: degradation and reactivation of damaged proteins. *Ann. Rev. Genet.* **27**, 437–496.
- [4] Barnes, J. A., Dix, D. J., Collins, B. W., Luft, C. & Allen, J. W. 2001 Expression of inducible Hsp70 enhances the proliferation of MCF-7 breast cancer cells and protects against the cytotoxic effects of hyperthermia. *Cell Stress Chaperon.* **6**, 316–325.
- [5] Wust, P., Hildebrandt, B., Sreenivasa, G., Rau, B., Gellermann, J., Riess, H., Felix, R. & Schlag, P. M. 2002 Hyperthermia in combined treatment of cancer. *Lancet. Oncol.* **3**, 487–497.
- [6] Hildebrandt, B., Wust, P., Ahlers, O., Dieing, A., Sreenivasa, G., Kerner, T., Felix, R. & Riess, H. 2002 The cellular and molecular basis of hyperthermia. *Crit. Rev. Oncol. Hematol.* **43**, 33–56.
- [7] van der Zee, J. 2002 Heating the patient: a promising approach? *Ann. Oncol.* **13**, 1173–1184.
- [8] Neznanov, N., Komarov AP, Neznanova, L., Stanhope-Baker, P. & Gudkov, A. V. 2011 Proteotoxic stress targeted therapy (PSTT): induction of protein misfolding enhances the antitumor effect of the proteasome inhibitor bortezomib. *Oncotarget* **2**, 209–221.
- [9] Molineaux, S. M. 2012 Molecular pathways: targeting proteasomal protein degradation in cancer. *Clin. Cancer Res.* **18**, 15–20.

- [10] Szymańska, Z. & Żylicz, M. 2009 Mathematical modeling of heat shock protein synthesis in response to temperature change. *J. Theor. Biol.* **259**, 562–569.
- [11] Peper, A., Grimbergen, C. A., Spaan, J. A., Souren, J. E. & van Wijk, R. 1998 A mathematical model of the hsp70 regulation in the cell. *Int. J. Hyperther.* **14**, 97–124.
- [12] Petre, I., Mizera, A., Hyder, C. L., Meinander, A., Mikhailov, A., Morimoto, R. I., Sistonen, L., Eriksson, J. E. & Back, R. 2011 A simple mass-action model for the eukaryotic heat shock response and its mathematical validation. *Nat. Comp.* **10**, 595–612.
- [13] Mizera, A. & Gambin B. 2010 Stochastic modelling of the eukaryotic heat shock response. *J. Theor. Biol.* **265**, 455–466.
- [14] Lepock, J. R., Frey, H. E. & Ritchie, K. P. 1993 Protein denaturation in intact hepatocytes and isolated cellular organelles during heat shock. *J. Cell Biol.* **122**, 1267–1276.
- [15] Abravaya, K., Phillips, B. & Morimoto, R. I. 1991 Attenuation of the heat shock response in HeLa cells is mediated by the release of bound heat shock transcription factor and is modulated by changes in growth and in heat shock temperatures. *Genes Dev.* **5**, 2117–2127.
- [16] Kwiatkowska, M., Norman, G. & Parker, D. 2011 PRISM 4.0: verification of probabilistic real-time systems. *Lect. Notes. Comput. Sc.* **6806**, 585–591.
- [17] Hucka, M., Finney, A., Sauro, H. M., Bolouri, H., Doyle, J. C., Kitano, H., Arkin, A. P., Bornstein, B. J., Bray, D., Cornish-Bowden, A. et al. 2003 The systems biology markup language (SBML): a medium for representation and exchange of biochemical network models. *Bioinformatics* **19**, 524–531.
- [18] Sung, M. H. & Simon, R. 2004 In silico simulation of inhibitor drug effects on nuclear factor-kappaB pathway dynamics. *Mol. Pharmacol.* **66**, 70–75.
- [19] Smith, B. J. & Yaffe, M. P. 1991 Uncoupling thermotolerance from the induction of heat shock proteins. *Proc. Natl. Acad. Sci. USA* **88**, 11091–11094.

- [20] Rieger, T. R., Morimoto, R. I. & Hatzimanikatis, V. 2005 Mathematical modeling of the eukaryotic heat-shock response: dynamics of the hsp70 promoter. *Biophys. J.* **88**, 1646–1658.
- [21] Gillespie, C. S., Wilkinson, D. J., Proctor, C. J., Shanley, D. P., Boys, R. J. & Kirkwood, T. B. L. 2006 Tools for the SBML. Community. *Bioinformatics* **22**, 628–629.
- [22] Shapiro, B. E., Hucka, M., Finney, A. & Doyle, J. 2004 MathSBML: a package for manipulating SBML-based biological models. *Bioinformatics* **20**, 2829–2831.
- [23] Charzyńska, A., Nałecz, A., Rybiński, M. & Gambin, A. 2012 Sensitivity analysis of mathematical models of signaling pathways. *BioTechnol.* **93**, 291–308.

Figure Legends

Figure 1.

Scheme of the HSR model. Squares represent species, including complexes, and dots represent reactions, with substrates and products denoted respectively by incoming and outgoing arrows. On the left side of the scheme, the denaturation of native proteins P and refolding or degradation of denatured proteins S (substrate) moderated by the HSP chaperones. On the right side, the adaptive HSP production loop, stimulated by HSF, which trimerise and initiate HSE transcription and HSP mRNA translation (dotted arrow). As a negative feedback, HSP molecules promote HSF trimers dissociation and inhibit single HSF molecules by direct binding. The loop is closed by the inflowing substrate which forces out inhibited HSF out of the complex with HSP.

Figure 2.

Numerical simulations of the HSR ODE model for a constant 42°C heating strategy. Simulation starts at a 37°C steady state. The upper plot depicts HSP response to the temperature-stimulated inflow of denatured proteins S (substrate). Free substrate is instantaneously bound into a HSP:S complex. Insufficient amount of free HSP causes its extraction from the HSP:HSF complex, forming an initiative response of the cell. Released in exchange HSF induces adaptive production of HSP molecules to complement its deficiency as indicated by accumulation of S, with peak at ca. 25 min. After over 120 min the excess of upregulated HSP is used to inhibit HSF activity. System completely stabilises after ca. 650 min (Fig. S1 in the Supporting Material) with most of constantly inflowing S secured in the HSP:S complexes. The lower plot depicts the adaptive HSP production, stimulated by HSF. HSF trimerises and initiate HSE transcription to mRNA, followed by further translation to HSP, as visible by the shifted activity of subsequent components.

Figure 3.

Thermotolerance in the heat-shock response: the substrate activity (solid) during the two consecutive immediate heat-shocks (dotted) of 5°C over the homeostatis level of 37°C. The intensity of intoxication resulting from the amount of substrate (filled area) depends on the time gap between heat-shocks. Interestingly, activity of the substrate in the second shock can be

even higher than activity in the first shock, as shown for the time gap of 240 min. This is due to a temporary deficit of HSP (see. Fig. S4 in the Supporting Material for details).

Figure 4.

The desensitisation coefficient \mathcal{D}_2 for the substrate in the ODE model (black line) and its mean and standard deviation in CTMC, plotted against the time gap between end of the first heat-shock and the beginning of the second heat-shock. Duration of both heat-shocks Δt_n ($n = 1, 2$) is equal to 71 min. Memory of the first heat-shock is lost when the desensitisation coefficient value stabilises around 0, which is approximately at 400 min for both mathematical models. Mean (yellow line) and standard deviation (orange line) of \mathcal{D}_2 was calculated at selected time points (dots). Both estimators have a confidence interval with 95% confidence level. In case of the mean value the confidence interval width is less than $5 \cdot 10^{-3}$, whilst for the standard deviation the confidence interval is depicted as a strip. Estimators were calculated using APMC with 10^4 and $5 \cdot 10^4$ independent simulation samples for the first and the second moment respectively (see Text S3 in the Supporting Material, Sec. 2 for details).

Figure 5.

The heat-shock response with respect to different temperatures and to different inhibition levels, applied separately (unimodal treatments) and simultaneously (combined treatment). The upper left plot depicts ODE trajectory of the substrate (solid lines) and the HSP:substrate complex (dashed lines), upon a 71 min heat-shock induced at 38 min for $T = 37, 38 \dots, 42^\circ\text{C}$. The upper right plot depicts the same trajectories for bortezomib maximum inhibition levels $I_{100} = 0, 20, \dots, 100\%$. In the similar manner the bottom left plot presents an effect of combining both therapies for varying T and fixed $I_{100} = 65\%$. Finally, the substrate toxic response coefficient \mathcal{R}_1 (Eq. 2) and the analogous coefficient for HSP:S, measuring HSR capacity, are depicted in the bottom right plot with respect to $T \in [37, 47]$, i.e. a continuous temperature range, broadened for a context. For a comparison \mathcal{R}_1 coefficient curves are presented for both a unimodal hyperthermia treatment (thin lines) and a treatment combined with $I_{100} = 65\%$ (thick lines).

Figure 6.

Contour plot of the heat-shock response level \mathcal{R}_1 with respect to a heat-shock temperature (vertical axis) and with respect to a maximum level of proteasome inhibition for heat-shock applied at $t_1 = 38$ min (left plot), or with respect to time of heat-shock application at maximum inhibition of $I_{100} = 65\%$ (right plot). Heat-shock takes $\Delta t_1 = 71$ min. Level of \mathcal{R}_1 (Eq. 2), denoted on the plot by colours from blue (the weakest) to red (the strongest), measures the toxicity of the combined therapy. Dashed vertical line at each plot denotes conditions for the other plot. Choice for maximum inhibition level I_{100} was driven by data reported in literature (see text for details), whereas choice for heat-shock time was based on maximisation of the multimodal strategy response (cf. right plot).

Figures

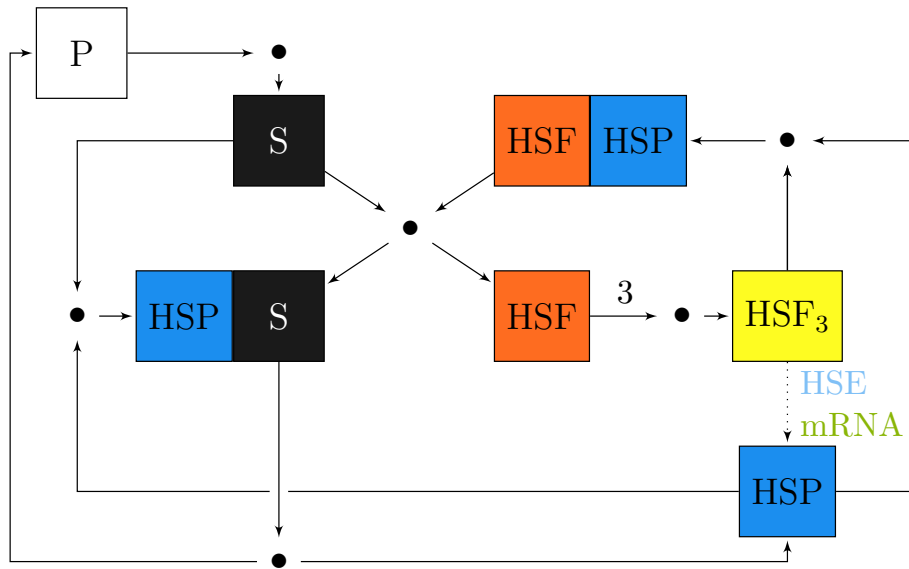


Figure 1:

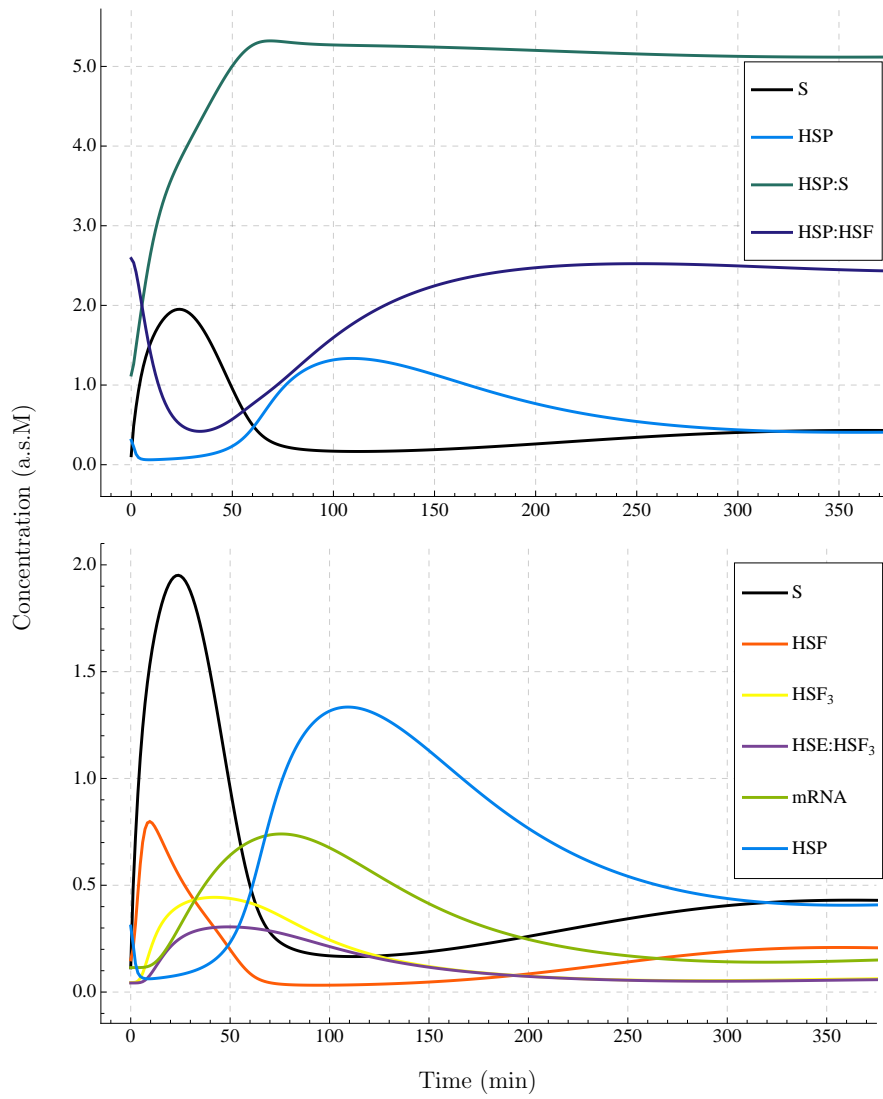


Figure 2:

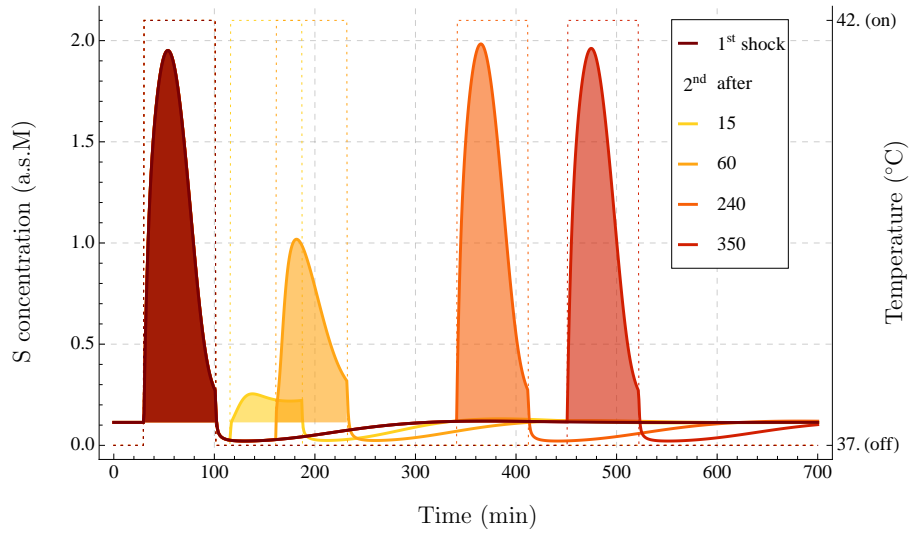


Figure 3:

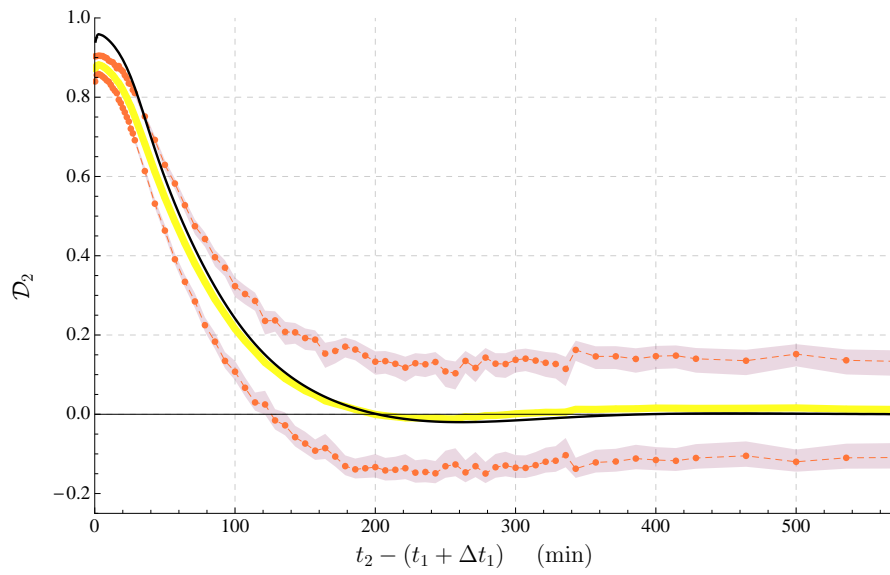


Figure 4:

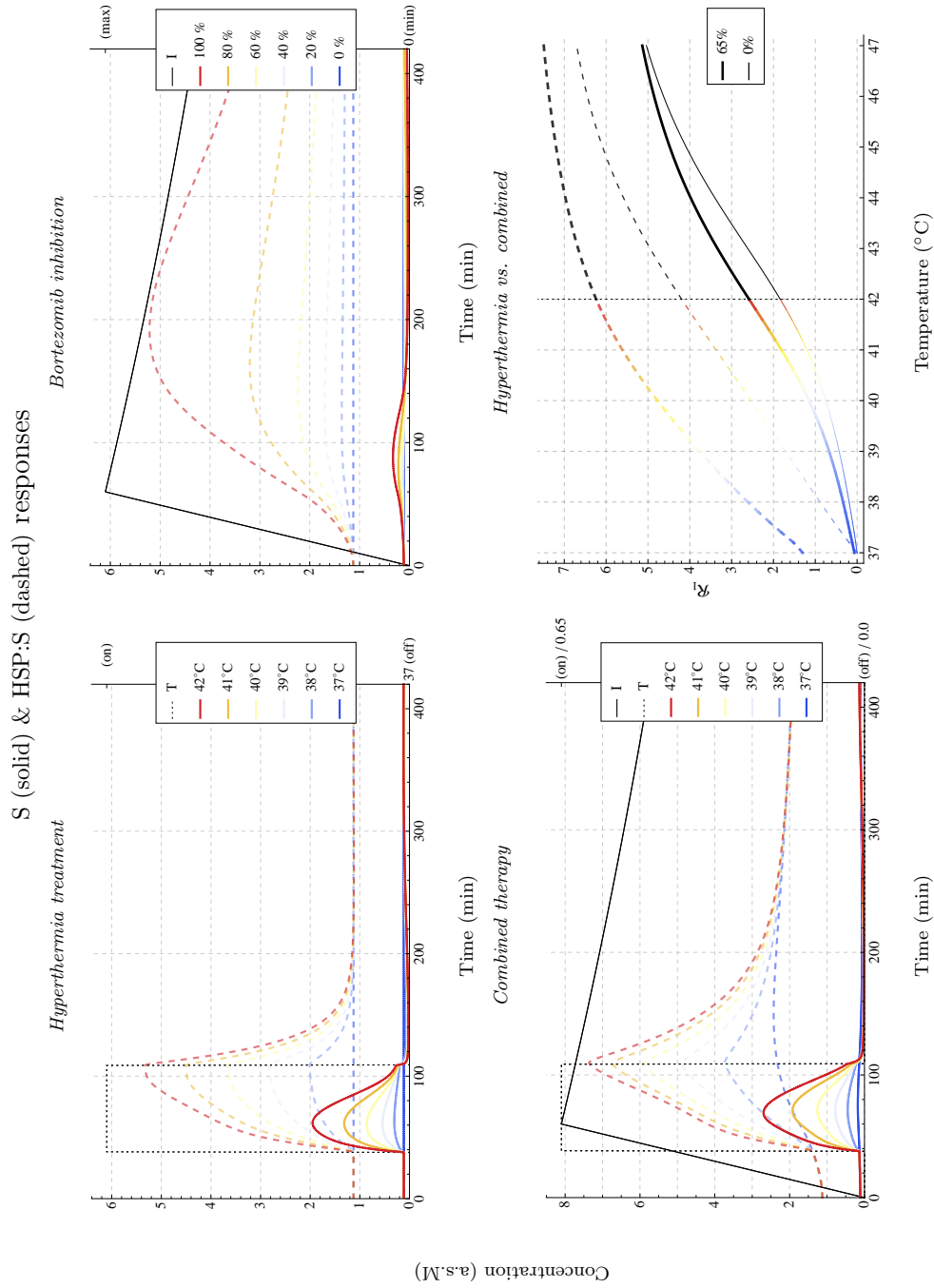


Figure 5:

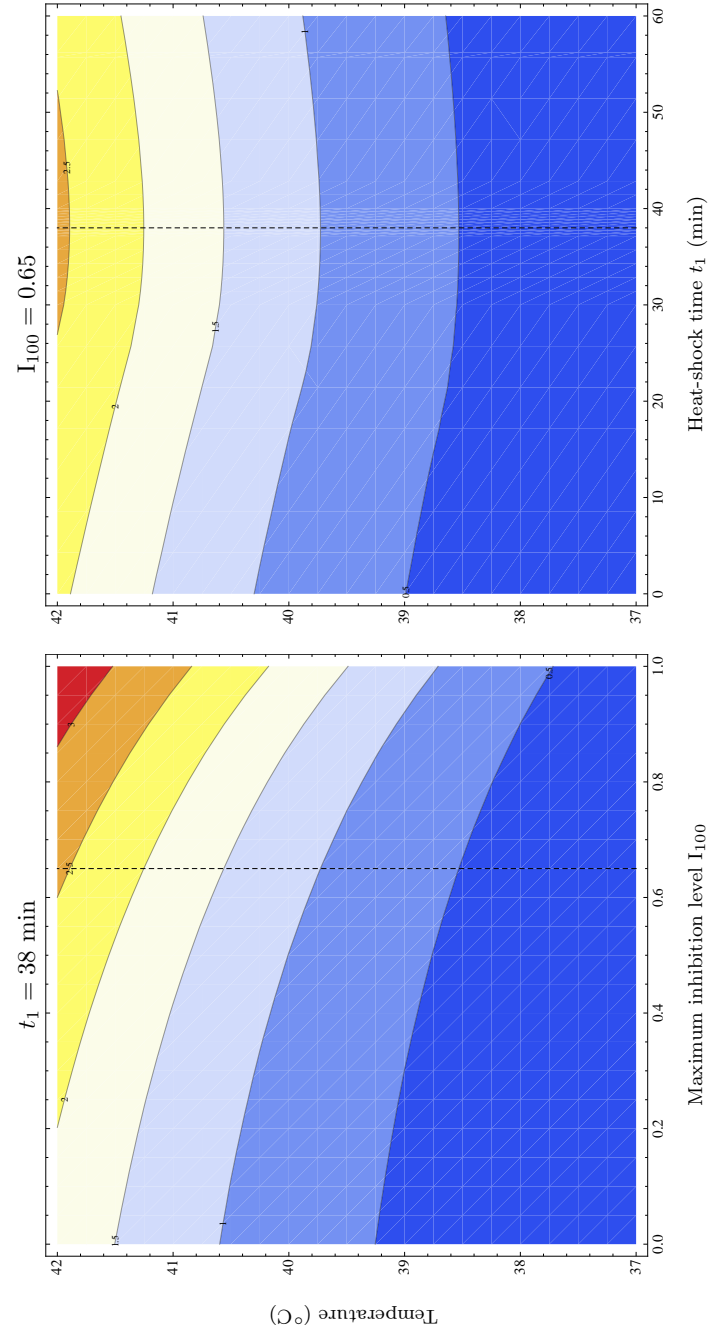


Figure 6:

Supporting Material index

Figure S1: Stability of the HSR ODE model.

Figure S2: The HSE:HSF₃ fit to the experimental data.

Text S3: Stochastic modelling of HSR

Figure S4: The substrate and HSP response to the two consecutive immediate heat-shocks.

Figure S5: Contour plots of the heat-shock response level for multiple equally-distributed heat-shock application times.

Figure S6: Area under the bortezomib inhibition curve (AUC) versus heat-shock application time.

Additional Files index

File F1: XML file in the SBML format containing deterministic model of HSR.

File F2: Text file in the PRISM model format containing stochastic model of HSR.